Research Square

Preprints are preliminary reports that have not undergone peer review.
They should not be considered conclusive, used to inform clinical practice,
or referenced by the media as validated information.

Features of on-site installation MAG process with M21 mixture and solid wire in applying to thick-sheet pearlitic structural steel for large-unit assemblies of nuclear power facilities

Andrei Paliakou

mortis2008@mail.ru

Belarusian-Russian University: Belorussko-Rossijskij universitet https://orcid.org/0009-0002-5293-2283

Dovlet Hemdemov

Middle East Technical University: Orta Dogu Teknik Universitesi

Artur Karatseyeu

Belarusian-Russian University: Belorussko-Rossijskij universitet

Research Article

Keywords:

Posted Date: November 9th, 2026

DOI: https://doi.org/10.21203/rs.3.rs-11201282/v1

License: This work is licensed under a Creative Commons Attribution 4.0 International License.
Read Full License

Features of on-site installation MAG process with M21 mixture and solid wire in applying to thick-sheet pearlitic structural steel for large-unit assemblies of nuclear power facilities

Andrei Paliakou, Dovlet Hemdemov, Artur Karatseyeu

Introduction

Nowadays mechanized arc welding process with $M21$ mixture and solid melting wire (hereinafter to as $MAG\ M21\ SOLID$) is being applied widely not only in factory conditions, but also for on-site installation works [1].

Compared with manual welding processes, high productivity and low required welder's qualification are being provided with successful $MAG\ M21\ SOLID$ process using for sheet metal with the aim of obtaining sufficient plastic non-defect butt and fillet welds, predominantly, in flat and "boat" position (including welding without backing strip; PA/PB positions). In such situations, meaningfully depending on severity of welding parameters and local overheating of metal, weld pool fluidity isn't being found as a determining factor that identify welding technique and torch manipulation in each separate welding pass (the root, filler, cap passes).

Over wide range of wire feed velocity (v_{WFV}) and arc voltage (U_A) that defined fact welding current (I_W) during display visualization in relating to welding machine control unit, as well as when there are frequent fluctuations of arc length (L_A), movement velocity and torch angle relative to normal to joint (v_T and α_T), in most cases, a welder is able to control the process of weld pool formation and movement. At the same time a welder cans promote the ratio "sufficient penetration depth (h_P) for base metal of welded details – stability process of wire metal melting – fact of confusion for these metals as arc travels".

However, practice shows that, under on-site installation conditions, as a rule, welders mainly apply the hard welding parameters instead of soft ones. It is being caused by necessity of welding in overhead and flat positions (hereinafter to as $PE/PD/PF$ positions) with extremely difficult control of increased fluidity weld pool due to gravitational force influencing to that one. In turn, it increases significantly possibility of non-penetration relating to metal of edges and between weld beads in the passes.

This situation is being exacerbated by the fact that welders apply for $MAG\ M21\ SOLID$ synergic adjustments of the flux wire, when for the comparable wire feed velocity and arc voltage difference in provide amperage is being risen to $50\ A$ and more, but on the lower side (as, for instance, in the control units of $LINCOLN\ SPEED\ TEC\ 400/500$ welding machines).

As a result, during such $MAG\ FCAW$ (the flux wire) welding parameter's adjustment instead of $MAG\ SOLID$ (solid wire), the welding parameters is being become further softening. However, value of the welding current is being detected to diminish to $115 - 120\ A$, and typical clearly audible sound of arc metal transition is being disappeared almost.

This leads to almost non-avoid periodic non-penetrations of the metal because under such conditions slowing down welding speed (v_W) and the shortest arc, in summary, aren't able to compensate for extreme low power of such arc discharge and, correspondently, welding heat input. In many cases this situation is perplexed by low-quality inter-pass cleaning of the metal from slag, and areas of contaminations transform to weld discontinuities that easily having identified by ultrasonic control method (hereinafter to as UT).

Additionally, in relation to $MAG\ M21\ SOLID$, literature hasn't had recommendations yet for adequate calculating of approximate values of the arc voltage regarding the wire feed velocity being selected, that is being found to measure up for counted value of current density (γ) depending on cathode current load and corresponding deposition coefficient (α_D) $[2 - 6]$.

The data that is being found to present for low-carbon low-alloy steel welding in pure carbon acid, concerning both solid and flux wires, isn't suited to $MAG\ M21\ SOLID$ process since physical-chemical characteristics of gas atmospheres are different considerably.

The observations show that welders don't apply synergetic welding parameters ratios for $MAG\ M21\ SOLID$ process using $LINCOLN\ SPEED\ TEC\ 400/500$ welding machines. Under

conditions of these settings, the welding wire is found to melt non-uniformly and inconsistently, with characteristic cracking sound. It's being involved to witness about balance violation between values of the welding current and arc voltage during feeding and melting processes of the welding wire, especially for its wire stick-out (L_W) for about $18\ mm$ and more if there is an absence of access regarding bottom points in narrow deep groove preparation.

It should be noted that there are features of initial joint assembly before on-site installation welding when uniformity of bevel angle (α_B) and the root opening (b) between details is being found to be critical important. The fact is that there are two mutual-excluding factors here. From the first side, for the joint assembly before welding, it's necessary that the required root opening is being identified to set regarding its sufficiency in relation to metal penetration of weld root face. From the other side, distance between the top edges of the groove preparation is being detected to increase extremely, due to locksmith mistake in the bevel angle toward higher values. Such locksmith mistake is called "higher angle of edge opening".

Under conditions of urgent on-site installation assembly-welding, relating large-unit massive factory incoming nodes of $U-shaped$ load-bearing base on fuel element transportation portal at nuclear power plant reactor building (hereinafter to as NPP), a welder does not have an opportunity to correct the bevel angle with implementing of the consequent repeat assembly in concern to portal load-bearing base under supervision of surveyors. The portal load-bearing base is responsible structure with a mass exceeding $180\ tonnes$, a height exceeding $25\ m$, a metal thickness of up to $40\ mm$ ($Figure\ 1a$). In cases of violation in the edge groove preparation symmetrizing (as, for instance, in $TJ83.3$ joints ($ISO\ 9692-1$) with the groove preparation being characterized by the non-standard non-symmetric narrow deep), it forces to start welding exactly from PD position because of ($Figure\ 1b$):

1. Regarding root pass welding in flat position, wire stick-out can be constituted more than $18\ mm$ since the groove preparing obstacles for the nearest torch accommodation.

2. As a result, under the given hard welding parameters, value of the welding current is being identified to diminish from $180-185\ A$ to $150-155\ A$. An arc commences lazing around in the groove preparation, and there is the maximum risk of root infusion's appearance in the edges (especially in case the exceeded speed of the manipulation).

3. In flat position the welding current is being detected to stabilize gradually till level for about $180-185\ A$, but only if there is a step-by-step increase of filler layer height during deposition of every filler pass.

$Figure\ 1(b)$ shows the following layers: №1 – root (PD position); №2 – filler (PB position); №3 – cap (PB position); №4 – backing weld (filler-cap of weld root) (PD position; stringer beads, as used for the main capping layer).

It should be noticed that, considering thick-plate workpieces that are produced using $S355J2W$ pearlitic structure steel $20-40-mm-sick$, for such butt and fillet welds, the actual capping layer width (B_C) is able to exceed dimensions that are being recommended by $ISO\ 9692-1$. But it isn't significant in terms of such weld's exploit characteristics.

However, if an edge's opening angle had been broken to the lower side, for the high-described extremely soft welding parameters:

a) it's extremely difficult and, in more cases, impossible, to provide penetration of the weld root via relatively low-ampere arc, especially in $PE/PD/PF$ welding positions, the low bevel angle and the root opening.

b) penetration depth is minimum for the root, filler and cap pass (on the order of tenths of a millimeter), and that's unacceptable concerning such responsible welds even if there is a seeming simplicity of welder's providing with requirement the cap layer geometry.

Therefore, based on high-present review, an analysis of features is a highly relevant task regarding on-site installation $MAG\ M21\ SOLID$ of thick-plate pearlitic structure steel on large-unit assemblies in nuclear power facilities (with development of recommendations in the welding parameters, technique and manipulations).

Materials and equipment

The research was conducted using the following equipment and materials:

- $LINCOLN\ SPEED\ TEC\ 400\ PF$ welding machine (MAG).
- $G3Si1$ bare welding solid wire with a diameter value of $1.2\ mm$ (d_W).
- M21 shielding gas mixture ($80\%Ar\ +\ 20\%CO_2$).
- $S355J2W$ sheet pearlitic structure steel with a thickness of $16, 20, 30\ mm$.
- ultrasonic flaw detector of the certification center.

It was considered $BJ1.5$, $TJ83.3$ and $BJ1.3$ joints ($ISO\ 9692-1$).

Main research

Initially, from common-known reference wide ranges for concentration of emission electrons within the gas arc discharge (n_E; $10^{16} - 10^{17}\ particles/cm^3$ of the arc) and root-mean-square electron velocity (v_E; $10^5 - 10^6\ m/s$) (typical for $MAG\ M21\ SOLID$ with wire diameter of $1{,}2\ mm$) [7], it was suggested determining via count-experiment method more precise estimated values of these parameters for the cathode current load within the range of $180 - 130\ A$.

Under on-site installation conditions, this is a limit range that is used by welders in $PE/PD/PF$ positions in terms of success achievement from weld pool processes implying its fluidity, formation and movement.

To attain this goal successfully, the following methodology was offered:

1. It was written well-known formula for calculating of the current density (γ_A) in the gas arc discharge through n_E and v_E parameters (omitting heavy ions and neutral particles):

$$\gamma_A = n_E \cdot e \cdot v_E, \tag{1}$$

where γ_A – current density within the gas arc discharge, A/mm^2.

n_E – concentration of electrons within the gas arc discharge with certain volume, $particles/cm^3$.

e – elementary charge ($1{,}6 \cdot 10^{-19}\ A \cdot s$).

v_E – root-mean-square electron velocity in the gas arc discharge, m/s.

2. The following initial conditions of calculating were figured out:

- making up for manual arc welding with coated melting electrode (hereinafter to as $SMAW$), *MAG M21 SOLID* is being found to characterize more current density and more arc temperature and, consequently, more cathode emission capability (the weld pool is a cathode for direct current in negative polarity).
- it is assumed that n_E and v_E values are being increased proportionally according to rise of the cathode current load, and this commensurate increase can be expressed by uniform coefficient for ease-of-use concerning calculating of the welding parameters under on-site installation conditions.
- for clarification procedure of the deposition coefficient as the cathode current load increases, arc voltage value of $20{,}0\ V$ was accepted as baseline value. For trial depositions, values of the wire feed velocity were being conformed to $5{,}2$ and $3{,}3\ m/min$ while 180 и $130\ A$ current values were being displayed in the control unit. It's the base welding parameters.

3. For welding current values of 180 and $130\ A$, using the base welding parameters with video recording in relating the process of trial joint welding, it was defined diameter (d_A) and volume (V_A) of the cylindric arc with lengthen of a $0{,}5\ cm$ (the short arc): $d_A = 0{,}4\ cm$; $V_A = 0{,}0628\ cm^3$.

4. It was calculated the required current density (γ) via simplified formula applying values of cross-sectional area of the wire (S_W) and welding current.

5. Values of the current density were inserted into formula (1) for counting of this parameter.

6. From wide ranges of n_E and v_E values, it was determined the only approximate value for each this parameter, taking into account an assumption about proportionality of its commensurate increase as an current load increase in relation to the cathode.

7. During the trial depositions with the base welding parameters using, it was identified approximate values of the deposition coefficient for values of the welding current 180 and 130 A (15,4 and 13,5 $g/(\mathrm{A} \cdot h)$). This action afforded to define rise of the approximate deposition coefficient for the cathode current load increased in increments of 10 A: 0,2 − 0,5 ($g/(A \cdot h)$).

8. Figuring in approximate values of the deposition coefficient, it was computed values of the wire feed velocity.

9. For manual separate adjustment of parameters in the control unit, it was being identified values of the wire feed velocity and arc voltage for the base welding parameters (20,0 V).

10. For selected consumption of shielding mixture (19 l/min) in relation to 16, 20 and 30 mm metal thickness, a series of experimental welds on $BJ1.5$, $TJ83.3$ and $BJ1.3$ joints (root, filler and cap passes) was being implemented in overhead position, applying value of the arc voltage fine adjustment of control switch in real time mode (in both directions, upward and downward).

11. At the specified welding current that was displayed in the control unit, value of the arc voltage was found to register with the nearest tenth of a volt. This depended on criterion according to the onset of moment to steady and stability process in relation to wire metal melting process (visually and orally) accompanied by a simultaneous achievement of sufficient penetration depth value viewed visually.

12. Through the trial depositions, values of the deposition coefficient were clarified thanks to the welding parameters with received values of the wire feed velocity and arc voltage.

Thus, concerning the solid wire with a diameter value of 1.2 mm, it was identified approximate values of n_E and v_E parameters in imply to the cathode current load in range from 180 till 130 A ($Table$ 1).

$Table$ 1 – Emission characteristics of the cathode for different current load

I_W, A	$n_E, \cdot 10^{16}\ particles/cm^3$	$v_E, \cdot 10^5\ m/s$	$\gamma, A/mm^2$
180	*3,98*	*3,98*	*159*
170	*3,87*	*3,87*	*150*
160	*3,76*	*3,76*	*142*
150	*3,64*	*3,64*	*133*
140	*3,52*	*3,52*	*124*
130	*3,38*	*3,38*	*115*

Below there are represented calculated values of the wire feed velocity, clarified values of the deposition coefficient and experimentally determined values of the arc voltage that correspond to above-mentioned emission characteristics of the cathode ($Table$ 2).

$Table$ 2 – Welding parameters for different current load

I_W, A	$v_{WFV}, m/min$	$\alpha_D, {}^{g}/_{(A \cdot h)}$	U_A, V	$q_{M21}, l/min$	
180	*5,2*	*15,4*	*18,8*	*19*	*Torch incline angle to the normal to the joint is* 25°. *Wire stick-out not more than* 18 *mm.* *Zero root face on the prepared workpiece.*
170	*4,8*	*15,1*	*18,4*		
160	*4,4*	*14,7*	*18,0*		
150	*4,0*	*14,2*	*17,6*		
140	*3,6*	*13,7*	*17,2*		
130	*3,3*	*13,5*	*16,8*		

Taking into attention defined values of the arc voltage, it was being found to propose the empirical ratio «I_W–U_A» formula to MAG M21 $SOLID$ process (the coefficient of determination is equal to 1, the mean approximation error is 0%):

$$U_A = 40 \cdot 10^{-3} \cdot I_W + 11{,}6\ (V) \quad (2)$$

Regarding the root opening of at least 3 mm, zero root face on the prepared workpiece and the wire stick-out not exceed 18 mm, above-showed formula fully reflects relationship between variables of the welding current and arc voltage in relation to MAG M21 $SOLID$ process within the specified range of the current load of $180 - 130\ A$, and it's being involve highlighting principal difference from MAG 100% CO_2 $SOLID$ process (welding in pure carbon dioxide) – arc burning in the $M21$ shielding mixture is characterized by a low arc voltage.

Next, it was proposed to divide the welding parameters into two conventional groups depending on value of the welding current:

1. Hard welding parameters ($180 - 150\ A$, inclusive). 2. Soft welding parameters ($150 - 130\ A$, inclusive).

Ten welders with different levels of qualification tested two from the determined welding parameters on $BJ1.5$ joints (metal thickness of $20, 30\ mm$, groove angle of $38 - 42°$, root opening of $3\ mm$), using welding of root, filler and cap passes in $PE/PD/PF$ positions:

- $180\ A, 5{,}2\ m/min, 18{,}8\ V$ (the hardest welding parameters);
- $130\ A, 3{,}3\ m/min, 16{,}8\ V$ (the softest welding parameters).

The hardest welding welding parameters was successfully found to suit root, and filler passes independently from its quantity, and this one was recommended to apply under on-site installation conditions with following recommendations concerning the welding parameters and manipulations:

a) crescent-shaped weaving movements are required for each weld pass independently from its type. The weld beads in these passes are not stringer beads but extend across the entire width of groove ($Figure\ 2$).

b) the only width of the manipulation (W_m), depending on edge line of the current pass, is being found to change.

c) regarding curve-line sections of trajectory, minimum step is $h = 2\ mm$ for the arc diameter value of $4\ mm$. This ensures a minimum overlap of $2\ mm$ between adjacent arc coverage zones along the crescent-shaped weaving trajectories. Also, it provides with each subsequent section of the trajectory overlaps preceding section and produces a heating of the metal to 650 °C minimum value along the arc travel path.

d) time delays from 0,5 to 1,0 s are mandatory at for extreme positions of the trajectory. This guarantees value of the penetration depth at least 3 mm, facilities more uniform height of the pass bead and reduces labor requirements of the inter-pass cleaning. It should be noted that the term "undercut" is strictly inapplicable in this context considering the edges of top part for the root and filler passes since, in comparison with the cap layers, all the areas of edge depressions will have been effectively melted and filled by metal of subsequent filler or cap passes.

e) concerning the manipulations, the velocity on curve-line sections of the trajectory must constitute of $6 - 8\ mm/s$, and this corresponds with acceptable fluidity of weld pool metal (look at justification below).

f) torch incline angle, relating to the normal of the joint, should not exceed 10°, 30°, 45°, respectively, for the root pass, filler and cap ones. Regarding the root pass, it ensures quality penetration of the weld root (root dentation) ($Figure\ 3$), for filler passes – additional overview and control in imply to weld pool movement, for cap passes – it minimizes the risk in undercut formation for facing surface metal of the welded details after the edge overlap finishing, and it stops an extreme rise of the bead ($Figures\ 4, 5$). At the same time welders must accommodate directly opposite the welded joint (in PE position – along the longitudinal edges).

g) after every pass, it's necessary to produce uniform volume cleaning-excavation of the metal from slag to achieve metallic luster. This ensures uniform filling of the groove in height while the metal of filler passes is approaching to place of start, concerning deposition of the future capping layer.

The softest welding parameters was successfully found to suit the cap layer independently from the quantity of passes, and it was recommended to apply with the same clarifications like for root and filler passes (look at $a - f$ paragraphs above), excluding g paragraph, that is being found to apply here under the following formulation:

- after finishing in relation to the uniform volume cleaning-excavation of the last filler pass, it shouldn't exceed up to $2\ mm$ concerning distance between the bottom point of the cleaning and facing surfaces of the welded details (for the root back-side welding – not exceeding $3\ mm$). This guaranties not only the cap layer deposition without exceeding its geometry that is required but excepts possibility of metal undercut formation regarding facing surfaces of the welded details while the welding arc is delaying in extreme points of its movement trajectory. At the same time, the cleaning-excavation shouldn't be characterized by $\Pi - shaped$ configuration (including the root back-side welding). The reason is that under condition of the increased welding speed, it's being involved to exist the high risk that the arc won't have time to melt difficult-to-access points in bottom of excavation ($Figures\ 6, 7$).

These two welding parameters ($180\ A$ – root and filler pass; $130\ A$ – cap passes) were approbated applying welding in $PF/PE/PD$ positions in relation to $BJ1.3$ joints (metal thickness of $16\ mm$, groove angle $36 - 47°$, the root opening of $3\ mm$) and $TJ83.3$ joints ($30\ +\ 20\ mm$, $42 - 47°$, $3\ mm$):

- the soft welding parameters ($130\ A$) was being found suitable to root back-side welding for $BJ1.3$ joints with the one pass making after its thorough cleaning-excavation ($Figure\ 8$).

- the hard welding parameters ($180\ A$) was being found suitable to all passes for $TJ83.3$ joints, including stringer passes without manipulations in width ($Figure\ 9$).

In relation to base of the NPP portal structure, after welding of on-site installation $BJ1.5$ and $TJ83.3$ joints in PF and combined $PE - PA - PE/PD - PB - PD$ positions (sheet thickness of $20 - 40\ mm$, summary sheet length of $91\ meter$), applying proposed the hard ($180\ A$; root, filling) and soft ($130\ A$; capping) welding parameters, it was obtained the following result of UT control: no defects were detected in the welds comprising $6 - 18$ passes deposited using back-step sequence from the center toward the edges in 350-mm-long sections (total number of starts and stops in the passes was at least 1300) ($Figure\ 10$).

No defects were detected in *BJ1.3* control welding joints during the attestation process concerning ten welders (PE/PF positions) for the same welding parameters.

Based on estimation of approximate instantaneous cooling rate regarding weld metal and metal of heat-affected zone (hereinafter to as HAZ), for temperature of finished stage in reverse austenite-pearlite transformation ($750\ °C$), applying limiting-state model of continuously moving point heat source on surface of semi-infinite body (figuring in elevated thickness and thermal mass of the welded components of the nuclear power plant portal structure), below there is presented a justification concerning applicability of arc travel speed of $6 - 8\ mm/s$ (v_{CURVE}) on curve-line sections of the trajectory ($Table\ 3$) [7, 8]:

1. It was written formula for calculating the instantaneous cooling rate of the metal (ω):

$$\omega = -2 \cdot \pi \cdot \lambda \cdot \frac{(T - T_I)^2}{q / v_{CURVE}} \left(\frac{K}{s}\right) \quad (3)$$

where $\lambda = 0{,}38\ {}^{W}/_{(cm \cdot K)}$ – thermal conductivity of steel being welded.

$T = 1053\ K$ – temperature for the point of definition the ω value being required ($750\ °C$).

T_I – initial metal temperature at the given point immediately before the arc reaches it, K.

q – effective arc thermal power, W.

$v_{CURVE} = 0{,}7\ cm/s$ – welding speed (the arc travel speed on curve-line sections of its movement trajectory).

2. The value of effective arc thermal power and welding heat input per unit length ($^{q}/_{v_{CURVE}}$) were determined for the hard and soft welding parameters, after that the formula (2) was rewritten. For calculating, arc efficiency was taken as 0.8.

3. To minimize the risk of martensitic–bainitic microstructures, and, correspondingly, cold crack formation from weld and HAZ, the normal instantaneous cooling rate should be $10\ K/s$. Therefore, further it was determined the required initial metal temperature at the given point immediately before the arc reaches it (T_I).

4. For the instantaneous cooling rate of $30\ K/s$, it was recalculated the initial metal temperature for permissible increased heat dissipation from welding zone.

$Table\ 3$ – The calculating of the metal instantaneous cooling rate with the welding speed of $0{,}7\ cm/s$ considering the softest ($130\ A$; $16{,}8\ V$) and hardest ($180\ A$; $18{,}8\ V$) welding parameters

Calculation parameter	***The required metal instantaneous cooling rate for the point of approximate completion concerning reverse austenite-pearlite transformation (T = 1053 K; 750 °C)***	
	$\omega = 10\ K/s$	$\omega = 30\ K/s$
q_{130A}, W	1747	
q_{180A}, W	2736	
$q_{130A}/v_{CURVE}, J/cm$	2496	
$q_{180A}/v_{CURVE}, J/cm$	3909	
T_I^{130A}, K	921 (648 °C)	846 (573 °C)
T_I^{180A}, K	895 (622 °C)	801 (528 °C)

Thus, to obtain values of the metal instantaneous cooling rate in $10 - 30\ K/s$ values that facilitate sufficient plastic pearlitic structure of the weld and HAZ, the initial metal temperature should be at least $650\ °C$ for each consequent curve-line section of the arc travel trajectory relating to the crescent-shaped torch manipulation from edge to edge (along entire groove width).

Such preheating is being ensured by a minimum step of the crescent-shaped trajectory ($2\ mm$), being recommended in the article, with having for about $2\ mm$ value mutual overlap concerning the trajectory curve-line sections (see $Fig.\ 1$).

At the same time, trajectory extreme points also are being preheated to temperature at least $650\ °C$ due to the delays of the arc in these areas for about $0{,}5 - 1\ s$. The bright yellow incandescence of plastic metal during its crystallization.

Conclusions

1. For mechanized arc welding with $M21\ mixture$ and the solid wire diameter of $1.2\ mm$, it was suggested the methodology of calculating the wire feed velocity and arc voltage being required, based on the approximate value clarification in relation to cathode emission characteristics (free electron concentration and its root-mean-square velocity), for the cathode current load ranging of $180 - 130\ A$ (figuring in the current undercompensation effect) that is being applied by welders under on-site installation conditions in worked to the joints of $BJ1.5$, $TJ83.3$ and $BJ1.3$ pearlitic structural steels of increased thickness ($16 - 40\ mm$) (PE, PD, PF, PA, PB positions).

2. For mechanized arc welding with $M21\ mixture$, solid wire with a diameter value of $1.2\ mm$ and the cathode current load in the range of $180 - 130\ A$, it was proposed the empirical ratio «I_W–U_A» that is being found to differ from well-known formula for welding with pure carbon dioxide.

3. Regarding the root opening of at least 3 mm and zero root face on the prepared workpiece, it was determined and successfully approbated the hardest ($5{,}2\ m/min, 18{,}8\ V, 180\ A$) and softest ($3{,}3\ m/min, 16{,}8\ V,\ 130\ A$) welding parameters, recommendations of the welding technique, inter-bead cleaning features and the torch manipulation parameters, as well as welder action sequences being required for producing of root, filler and cap passes. Taken together, under conditions of on-site installation welding relating $BJ1.5$, $TJ83.3$ and $BJ1.3$ joints, it allows to ensure the penetration depth of the edge metal at least $3\ mm$ simultaneously with uniform and stable solid wire melting in consider to its diameter of $1.2\ mm$ and its stick-out not exceed $18\ mm$.

Conflict of Interest
The authors declare no competing interests.

Funding
No funding was received.

Author Contributions

Author 1. Paliakou Andrei.

A scientific and technical review of the problems associated with on-site installation MAG welding using a solid wire and an M21 shielding-gas mixture addressed in this study.

Development of a hypothesis concerning the proportional increase in the emission properties of the cathode — specifically, the concentration and root-mean-square velocity of emission electrons —as its current load increases under direct current, reverse polarity (MAG welding).

Development of a hypothesis concerning the applicability of a proportionality coefficient describing the increase in the cathode's emission properties with increasing current load to the rapid estimation of the approximate wire feed speed, welding current, and arc voltage under the current-load conditions most commonly applied by welders to the cathode, taking into account the current undercompensation effect. The proposed approach is applied to on-site installation MAG welding, using an M21 shielding-gas mixture and solid wire, of thick-section pearlitic structural steel in large-unit assemblies of nuclear power facilities.

Development of a methodology and determination of the principal MAG welding parameters using an M21 shielding-gas mixture and solid wire in accordance with the proposed hypotheses, for the wire diameter, arc length, and approximate arc volume considered in the study.

Analysis of the final results of the theoretical and experimental investigations, including formulation of conclusions.

Derivation of an equation describing the relationship between welding current and arc voltage for the cathode current-load range of 130–180 A.

Development of recommendations for MAG welders using an M21 shielding-gas mixture and solid wire concerning the principal welding parameters, welding technique, and sequence of operations.

Author 2. Hemdemov Dovlet.

Preparation of the equipment and materials for the experiments.

Successful experimental and production-scale validation of the hypotheses proposed by Andrei Paliakou under practical conditions at the world's largest construction site of the four-reactor nuclear power plant "AKKUYU") (Turkey, Reactor Unit № 2).

Author 3. Artur Karatseyeu.

Processing and analysis of the results of mechanical strength tests and ultrasonic quality inspection of the welded joints produced during the experimental investigations.

References

1. Ovchinnikov, V. V. *Tekhnologiya ruchnoy dugovoy, argono-dugovoy, poluavtomaticheskoy dugovoy svarki* [Technology of Manual Arc, Gas Tungsten Arc, and Semiautomatic Arc Welding]. Moscow: Akademiya, 2025, 288 p.

2. Koroteev, A. O. *Tekhnologiya dugovoy svarki konstruktsionnykh staley s dvukhstruynoy koaksial'noy podachey komponentov zashchitnoy gazovoy sredy* [Arc-Welding Technology for Structural Steels with Two-Jet Coaxial Delivery of Shielding-Gas Components]. PhD dissertation, Specialty 05.02.10. Mogilev, Belarus: Belarusian-Russian University, 2017, 236 p.

3. Sholokhov, M. A. *Issledovanie i razrabotka tekhnologii mekhanizirovannoy svarki v zashchitnykh gazakh staley s ponizhennym soderzhaniem vrednykh primesey* [Investigation and Development of a Technology for Mechanized Welding of Steels with Reduced Contents of Harmful Impurities in Shielding Gases]. PhD dissertation, Specialty 05.03.06. Yekaterinburg, Russia: Ural State Technical University—UPI named after the First President of Russia B. N. Yeltsin, 2009, 151 p.

4. Varukha, E. N. *Nagrev i plavlenie pri dugovoy mekhanizirovannoy svarke* [Heating and Melting in Mechanized Arc Welding]. DSc dissertation, Specialty 05.03.06. Rostov-on-Don, Russia: Don State Technical University, 1998, 442 p.

5. Kulikov, V. P. *Tekhnologiya svarki plavleniem i termicheskoy rezki* [Fusion-Welding and Thermal-Cutting Technology]. 2nd ed., stereot. Minsk, Belarus: Novoe Znanie, 2018, 461 p.

6. Akulov, A. I., Alekhin, V. P., Ermakov, S. I., et al. *Tekhnologiya i oborudovanie svarki plavleniem i termicheskoy rezki* [Technology and Equipment for Fusion Welding and Thermal Cutting]. 2nd ed., rev. and suppl. Moscow: Mashinostroenie, 2003, 560 p.

7. Frolov, V. V., Volchenko, V. N., Yampolsky, V. M., Vinokurov, V. A., et al. *Teoriya svarochnykh protsessov* [Theory of Welding Processes]. Moscow: Vysshaya Shkola, 1988, 559 p.

8. Karkhin, V. A. *Teplovye protsessy pri svarke* [Thermal Processes in Welding]. St. Petersburg, Russia: Izdatelstvo Politekhnicheskogo Universiteta, 2015, 571 p.

Abstract

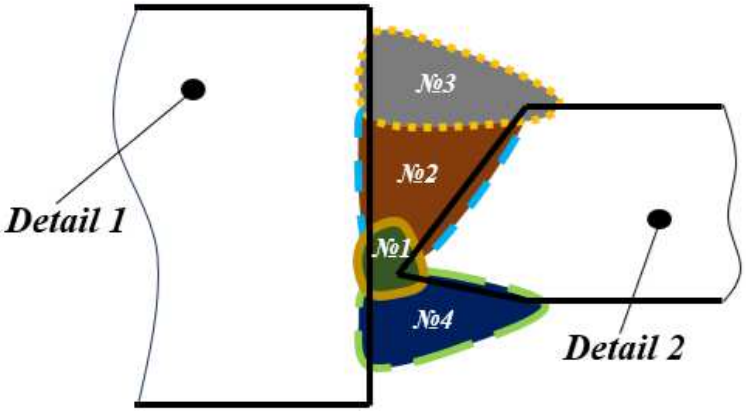
For the on-site installation welding being investigated, regarding the typically viewed the cathode current load in the range of $130 - 180\,A$ and taking into account the current undercompensation effect, the paper proposes an equation relating from welding current to arc voltage based on the premise that there is a commensurate comparable increase of emission electron characteristics that could be expressed via an approximate coefficient.

Keywords

On-site installation welding with gas mixture, electron emission characteristics, cathode current load, commensurate comparable increase of parameters, undercompensation effect, equation relating current to voltage, penetration depth, wire melting uniformity.

Figures





a) ***b***)

***Fig*. 1. Transportation portal at nuclear power plant reactor building (*a*) and *TJ*83. 3 joint with the non-symmetric narrow deep groove preparation (*b*) (the wire-out exceeds 18 *mm* for $\delta > 25$ *mm* in root pass (№1) and *PB* position)**

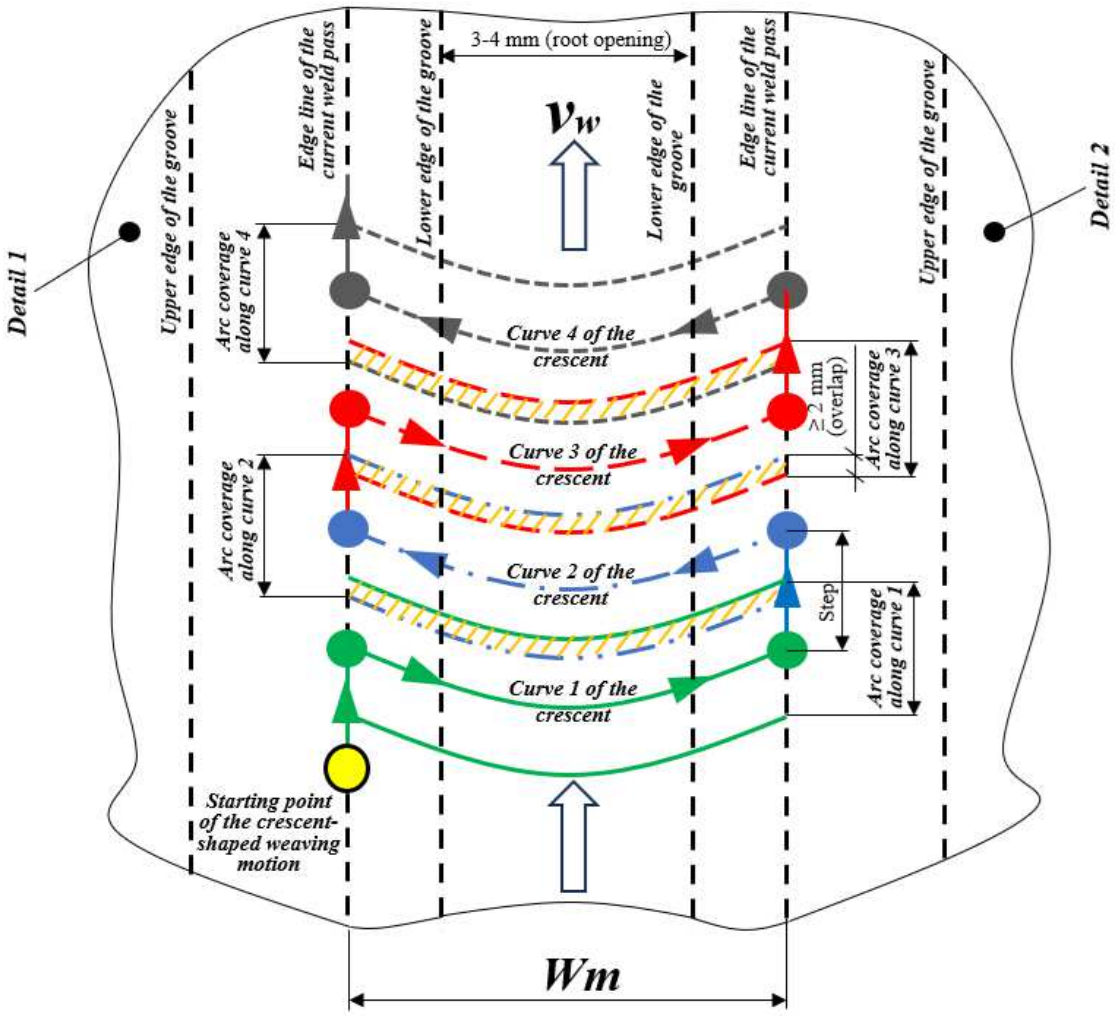


***Fig*. 2. The features in the trajectory of the arc manipulation for $PF/PE/PD$ positions**

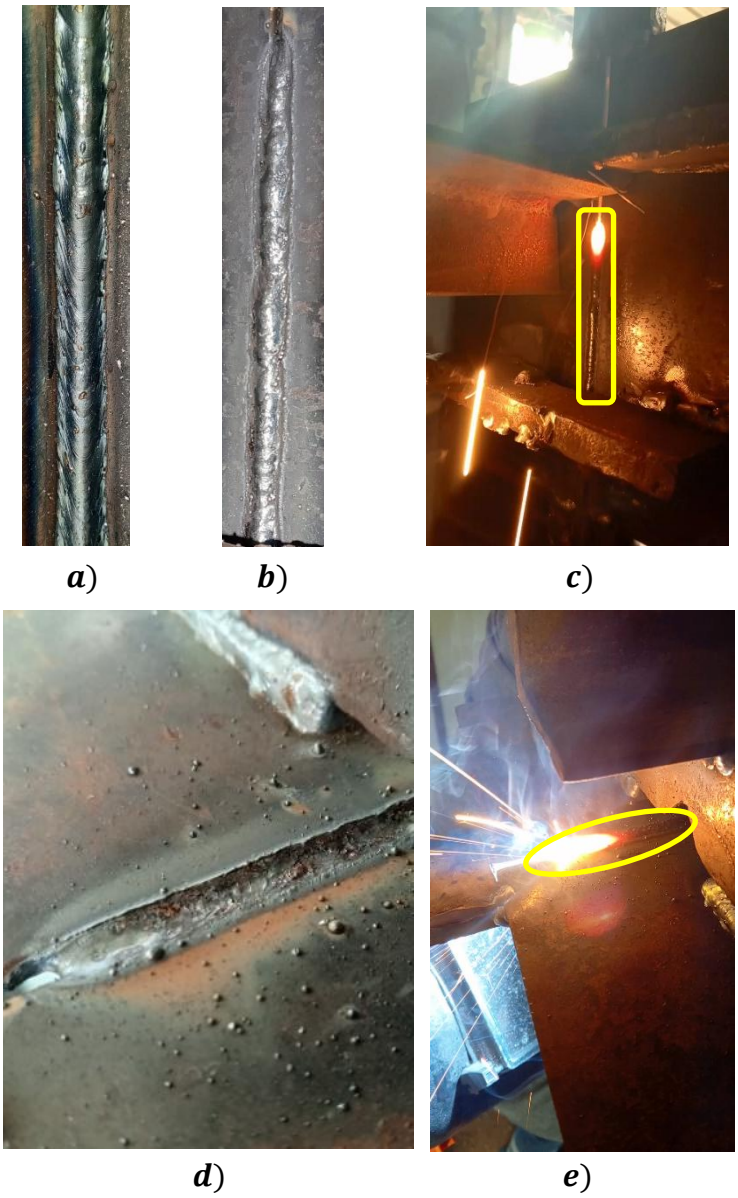


***Fig.* 3. Root pass (*a*) with back-side bead formation in *PF* position (*b*, *c*) and without that one in *PE* position (*d*, *e*) (*BJ*1. 3 joints)**

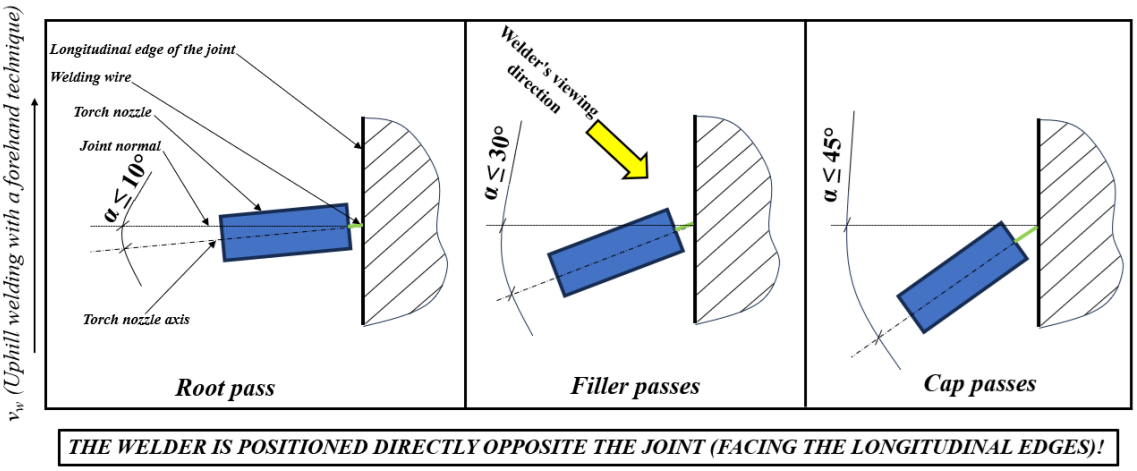


***Fig*. 4. Torch incline angle and the welding technique in *PF* position**

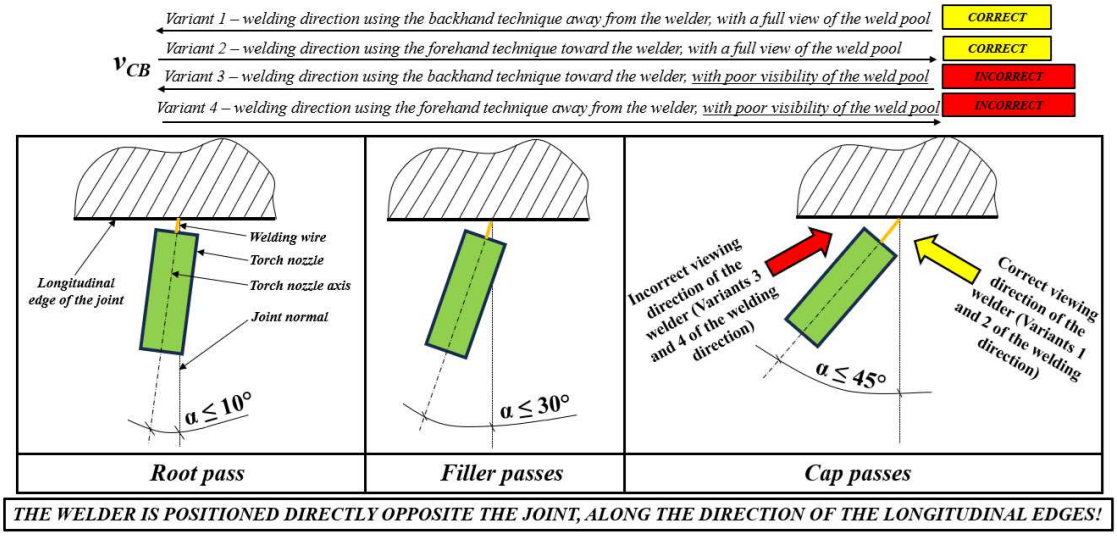


***Fig*. 5. Torch incline angle and the welding technique in *PE* position**

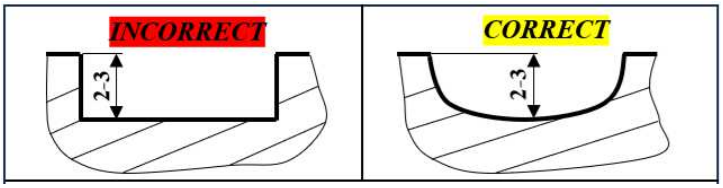
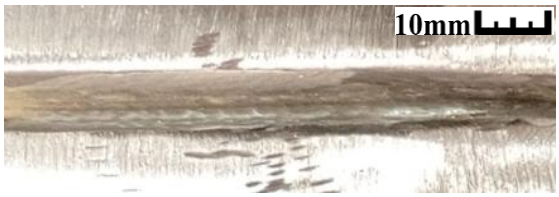


***Fig*. 6. Shape of the cleaning for the last filler pass (before capping)**



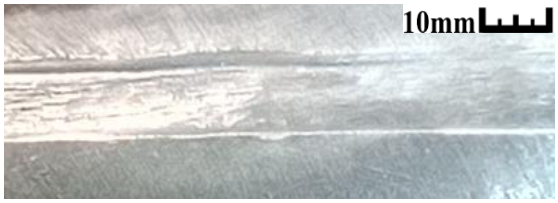
1. Root pass after welding (PE)



2. Root pass after cleaning (PE)



3. Filler pass after welding (PE)



4. Filler pass after cleaning before capping (PE)



5. Appearance of the root pass back-side (PA)



6. Deep cleaning-excavation of the root pass back-side (PA)



7. Root pass on the other side after welding (PA)



8. Root pass on the other side after cleaning (PA)



9. Filler pass after welding (PA)

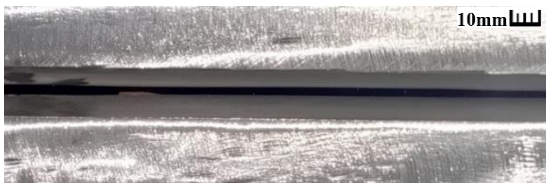


10. Filler pass after cleaning (PA)



11. Cap passes after welding and finished cleaning (PE and PA)

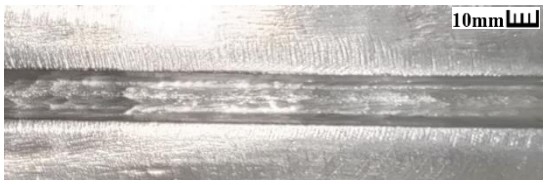
***Fig.* 7. Sequence of actions for *BJ*1.5 joint welding (20 + 20 *mm*) considering *MAG* M21 *SOLID* in combined position *PE/PA* with one filler pass and the soft welding parameters of the cap pass (suitable to *PE/PF* positions)**



1. Assembly with the root opening on the run-on and run-off tabs



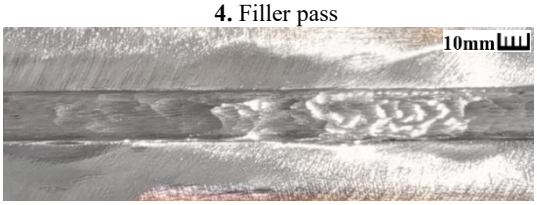
2. Root pass



3. Root pass after cleaning



4. Filler pass



5. Filler pass after the uniform-volume cleaning



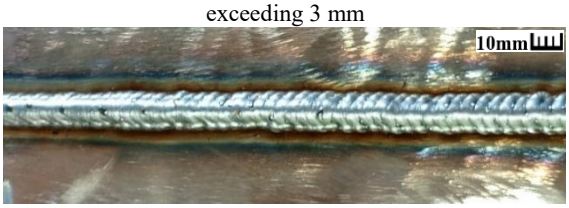
6. Cap pass



7. Cap pass after the slight final cleaning



8. Weld root cleaned from the reverse side to depth not exceeding 3 mm



9. Backing filler-capping pass deposited from the reverse side of the weld root



10. Backing pass after light cleaning

***Fig.* 8. Sequence of actions for *BJ*1.3 joint welding (16 + 16 *mm*) considering *MAG* M21 *SOLID* in *PE/PF* positions with one filler pass and the soft welding parameters of the cap pass**



1. The root opening (view from PB position)



2. Root pass (PD)
(view from PB position)



3. Root pass after cleaning on the other side from PB position



4. Stringer filler pass No. 1 along the groove edge adjacent to the thicker component (without groove) (PB)



5. Cleaning of the first filler stringer bead



6. Stringer filler pass No. 2 along the groove edge adjacent to the thinner component (with groove) (PB)



7. Stringer filler pass No. 3 along the groove edge adjacent to the ungrooved component (PB) (after cleaning)



8. Stringer filler pass No. 4 along the groove edge adjacent to the grooved component (PB) (after cleaning)



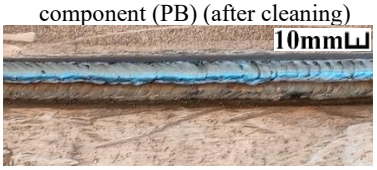
9. Cleaning of filler stringer bead No. 4



10. Stringer filler pass No. 5 along the groove edge adjacent to the ungrooved component (PB) (after cleaning)



11. Stringer filler pass No. 6 along the groove edge adjacent to the grooved component (PB) (after cleaning)



12. Stringer filler pass No. 7 along the groove edge adjacent to the ungrooved component (PB) (after cleaning)



13. Stringer filler pass No. 8 along the groove edge adjacent to the grooved component (PB) (after cleaning)



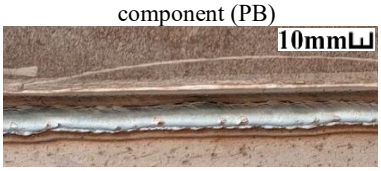
14. Final stringer filler pass (No. 9) along the groove edge adjacent to the ungrooved component (PB)
(after cleaning)



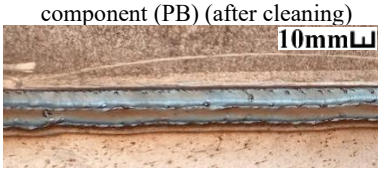
15. Cleaning of the final filler layer flush with the surfaces of the components (for capping)



16. Capping pass No. 1 along the groove edge adjacent to the ungrooved component (PB)



17. Capping pass No. 2 along the groove edge adjacent to the grooved component (PB) (after cleaning)



18. Capping pass No. 3 along the groove edge adjacent to the ungrooved component (PB) (after cleaning)





19. Capping layer after light finishing with a wire brush

***Fig.* 9. Sequence of actions for *TJ*83.3 joint welding (30 + 20 *mm*) considering *MAG* M21 *SOLID* in combined position *PD/PB/PD* with hard welding in all passes**



***Fig*. 10. Ultrasonic testing of the quality of *TJ*83. 3 welded joints: (*a*) ultrasonic inspection and (*b*) signal jump in the presence of defect**